Applied and Environmental Microbiology, July 2008, p. 4119–4132 Vol. 74, No. 13
0099-2240/08/$08.00+0 doi:10.1128/AEM.00229-08

Genomic and Functional Characterization of the Modular Broad-Host-Range RA3 Plasmid, the Archetype of the IncU Group▽†

Anna Kulinska,[1] Magdalena Czeredys,[1]‡ Finbarr Hayes,[2] and Grazyna Jagura-Burdzy[1]*

Department of Microbial Biochemistry, Institute of Biochemistry and Biophysics, PAS, 02-106 Warsaw, Poland,[1] and Faculty of Life Sciences and Manchester Interdisciplinary Biocentre, The University of Manchester, Manchester M1 7DN, United Kingdom[2]

Received 25 January 2008/Accepted 10 May 2008

IncU plasmids are a distinctive group of mobile elements with highly conserved backbone functions and variable antibiotic resistance gene cassettes. The IncU archetype is conjugative plasmid RA3, whose sequence (45,909 bp) shows it to be a mosaic, modular replicon with a class I integron different from that of other IncU replicons. Functional analysis demonstrated that RA3 possesses a broad host range and can efficiently self-transfer, replicate, and be maintained stably in alpha-, beta-, and gammaproteobacteria. RA3 contains 50 open reading frames clustered in distinct functional modules. The replication module encompasses the *repA* and *repB* genes embedded in long repetitive sequences. RepA, which is homologous to antitoxin proteins from alpha- and gammaproteobacteria, contains a Cro/cI-type DNA-binding domain present in the XRE family of transcriptional regulators. The *repA* promoter is repressed by RepA and RepB. The minireplicon encompasses *repB* and the downstream repetitive sequence r1/r2. RepB shows up to 80% similarity to putative replication initiation proteins from environmental plasmids of beta- and gammaproteobacteria, as well as similarity to replication proteins from alphaproteobacteria and *Firmicutes*. Stable maintenance functions of RA3 are most like those of IncP-1 broad-host-range plasmids and comprise the active partitioning apparatus formed by IncC (ParA) and KorB (ParB), the antirestriction protein KlcA, and accessory stability components KfrA and KfrC. The RA3 origin of transfer was localized experimentally between the maintenance and conjugative-transfer operons. The putative conjugative-transfer module is highly similar in organization and in its products to transfer regions of certain broad-host-range environmental plasmids.

Conjugative plasmids contribute greatly to the global spread of genetic information and gene exchange, as in some cases they can self-transfer even between distant bacterial species. Conjugative R factors assigned to the IncU incompatibility group have been isolated from a number of *Aeromonas* spp. and *Escherichia coli* strains from seawater fish hatcheries and diseased fish, as well as from clinical environments (2, 4, 6, 15, 26, 30, 31, 42). Members of the IncU plasmid group are implicated particularly in the dissemination of antibiotic resistance in *Aeromonas* strains associated with aquatic environments (15).

IncU representatives pAr-32 and pRAS1 contain resistance genes encoded within integrons, and on the basis of restriction enzyme analysis of both plasmid molecules, Sørum et al. (35) postulated a highly conserved backbone structure of IncU group members with variability in the region coding for antibiotic resistance. Similar observations were made with plasmids pASOT and pFBAOT (2, 26, 27). Plasmid pFBAOT6 (84,749 bp) has been sequenced recently and analyzed in silico (27). Plasmid Rms149 of the *Pseudomonas* IncP-6 group was assigned to the IncU group on the basis of incompatibility tests (12). Apart from homology between the replication genes of pFBAOT6 and Rms149, no conservation of the backbone structure was observed, in contrast to previous suggestions (11, 27).

As the main focus has been on their resistance gene cassettes, little is known about the biology of plasmids from the IncU group, of which RA3 is the archetype (3). This study describes the initial step in a complete functional analysis of plasmid RA3. First, the sequence of RA3 (45,909 bp) had to be established (accession no. DQ401103). It proved to be almost identical to pFBAOT6 in the backbone region. RA3 possesses a 10.5-kb antibiotic resistance region that contains a class I integron carrying *sulI*, *aadA2*, and *catA2* determinants. This differs from a similar insertion in pFBAOT6, the RA3 sequence possessing duplicated *sulI* and truncated *qac* genes in the 3′ conserved segment (3′CS). The insertion site of the integron in RA3 corresponds to the insertion site of the main variable region (54 kb) in pFBAOT6. Plasmid RA3 does not contain an IS*630* element, which in pFBAOT6 is inserted in the putative conjugative transfer region. Functional analysis demonstrated that RA3 was capable of high-frequency conjugal transfer to beta- and gammaproteobacteria, with a 1,000-fold lower frequency of transfer to alphaproteobacteria, revealing that the plasmid has a broad host range. The segregational stability of RA3 was confirmed in diverse bacterial host strains, the minimal region required for replication was defined, and the origin of conjugative transfer was localized.

* Corresponding author. Mailing address: Institute of Biochemistry and Biophysics, PAS, Pawinskiego 5A, 02-106 Warsaw, Poland. Phone: 48 22 823 71 92. Fax: 48 22 658 46 36. E-mail: gjburdzy@ibb.waw.pl.

‡ Present address: Department of Molecular and Cell Neurobiology, Nencki Institute of Experimental Biology, 02-093 Warsaw, Poland.

† Supplemental material for this article may be found at http://aem.asm.org/.

▽ Published ahead of print on 23 May 2008.

MATERIALS AND METHODS

Bacterial strains and growth conditions. The *E. coli* strains used were K-12 strains DH5α [F^- (Φ*80dlacZ*ΔM15) *recA1 endA1 gyrA96 thi-1 hsdR17* (r_K^- m_K^+) *supE44 relA1 deoR* Δ(*lacZYA-argF*)*U19*] (13), CV601 (*gfp* Rif^r Km^r), kindly supplied by K. Smalla (Braunschweig, Germany), and C600K (*thr-1 leu-6 thi-1 lacY1 supE44 ton-21 galK*) (23). *E. coli* C strain C2110 (*polA1 his rha*) (D. R.

TABLE 1. Plasmids used and constructed in this study

Plasmid	Relevant features	Copy no.	Reference or source
Used			
pAKE600	ori_{MB1} $oriT_{RK2}$ Pn^r *sacB*	High	7
pBGS18	ori_{MB1} Km^r	High	36
pET28	ori_{MB1} Km^r T7*p lacO* His_6 tag, T7 tag	Medium	Novagen
pET28mod	ori_{MB1} Km^r T7*p lacO* His_6 tag, T7 tag deleted, no BamHI site	Medium	G. Jagura-Burdzy
pGBT30	ori_{MB1} Pn^r *lacI*^{q} *tacp* expression vector	High	17
pGEM-T Easy	ori_{MB1}Pn^r	High	Promega
pPTOI	ori_{SC101} Km^r promotorless *xylE*	Medium	39
pUC18	ori_{MB1} Pn^r	High	43
RA3	IncU Cm^r Sm^r Su^r	Low	F. Hayes
Constructed			
pAKB1.101	pGEM-T with PCR product (6L2 and str7)[a] corresponding to 3,155-bp fragment of RA3		
pAKB1.102	pGEM-T with PCR product (inp5 and str7) corresponding to 1,261-bp fragment of RA3		
pAKB1.103	pGEM-T with PCR product (rep2 and str7) corresponding to 1,861-bp fragment of RA3		
pAKB7.5	pBGS18 with 460-bp HincII-BamHI fragment from RA3 (coordinates 9395–9854)		
pAKB9.5	pAKE600 with BamHI-PstI fragment from pAKB7.5		
pMOB1.4	pBGS18 with 2,563-bp PCR product (miniR1 and snaB2)		
pMOB1.5	pBGS18 with 327-bp PCR product (ant3 and ant2)		
pMOB1.5.1	pGBT30 with SacI-SalI fragment of pMOB1.5 to create transcriptional fusion *tacp-repA*		
pMOB1.6	pBGS18 with 1,409-bp PCR product (rep3 and rep4)		
pMOB1.6.1	pGBT30 with SacI-SalI fragment of pMOB1.6 to create transcriptional fusion *tacp-repB*		
pMOB1.7	pBGS18 with 362-bp PCR product (rep5 and rep7)		
pMOB1.7.1	pPTO1 with SphI-BamHI fragment of pMOB1.7 to create transcriptional fusion *repBp1/p2-xylE*		
pMOB1.8	pBGS18 with 312-bp PCR product (rep6 and rep7)		
pMOB1.8.1	pPTO1 with SphI-BamHI fragment of pMOB1.8 to create transcriptional fusion *repBp2-xylE*		
pMOB1.9	pBGS18 with 362-bp PCR product (rep1 and rep2)		
pMOB1.9.1	pPTO1 with SphI-BamHI fragment of pMOB1.9 to create transcriptional fusion *repXp-xylE*		
pMOB1.10	pBGS18 with 376-bp PCR product (ant1 and ant2)		
pMOB1.10.1	pPTO1 with BamHI fragment of pMOB1.10 to create transcriptional fusion *repAp-xylE*		

[a] Primers used in PCR.

Helinski, University of California San Diego) was used for minireplicon analysis. *Pseudomonas putida* KT2442 Rif^r was provided by C. M. Thomas (University of Birmingham, Birmingham, United Kingdom). *Agrobacterium tumefaciens* UBAPF2 (*gfp* Km^r Rif^r Sm^r) and *Ralstonia eutropha* 7MP228r (*gfp* Rif^r Km^r Pn^r) were kindly supplied by K. Smalla (Braunschweig, Germany).

Bacteria were grown in L broth or L agar (L broth with 1.5% [wt/vol] agar) at 37°C or 28°C (18) supplemented with appropriate antibiotics. For *E. coli*, we used benzylpenicillin sodium salt at 150 μg ml^{-1} in liquid medium and 300 μg ml^{-1} in agar plates for penicillin resistance, kanamycin sulfate (50 μg ml^{-1}) for kanamycin resistance, streptomycin sulfate (20 to 30 μg ml^{-1}) for streptomycin resistance, and chloramphenicol (10 μg ml^{-1}) for chloramphenicol resistance. For *R. eutropha*, *P. putida*, and *A. tumefaciens*, chloramphenicol (10 μg ml^{-1}) was used. L agar used for blue/white screening contained isopropyl-β-D-thiogalactopyranoside (IPTG; 0.1 mM) and 5-bromo-4-chloro-3-indolyl-β-D-galactopyranoside (X-Gal; 40 μg ml^{-1}).

Gene amplification. Standard PCRs (24) were performed with RA3 DNA as the template and the following pairs of primers: ant1 5′-C*GGATCC*GCGGGC CTGATCTATTGTTG-3′ (coordinates 45365 to 45384) and ant2 5′-C*GGATC CGCATGC*TTTCTATGCCGCTAACGGC-3′ (coordinates 45741 to 45722) for the *repAp* fragment, rep1 5′-C*GGATCC*CCGGAAACCAACTTGGCGGGC-3′ (coordinates 45750 to 45769) and rep2 5′-C*GGATCCGCATGC*CGCATAAAC TCGGCCTGT-3′ (coordinates 203 to 186) or rep5 5′-C*GCATGC*CCCCGGA AAACCAACTTGGCG-3′ (coordinates 45750 to 45769) and rep7 5′-C*GGATC C*GCCGCATAAACTCGGCCTGT-3′ (coordinates 203 to 186) for *repB1p*/ *repB2p*, rep6 5′-C*GCATGC*TTTCGGTGAGCTTGGCGGC-3′ (coordinates 45800 to 45818) and rep2 for *repB2p*, ant3 5′-C*GAGCTC*CACATCATTCTGA TGAGGGC-3′ (coordinates 45414 to 45433) and ant2 for *repA*, and rep3 5′-C *GAGCTC*TTGGCAAGTTAGGGGTGCAT-3′ (coordinates 45885 to 45904) and rep4 5′-CC*GTCGAC*GCCATCTAAACGGCTTTAC-3′ (coordinates 1385 to 1365) for *repB*. The restriction sites introduced for cloning are in italics. PCR steps were as follows: an initial denaturation at 95°C for 5 min and then 30 cycles of denaturation (95°C for 30 s), annealing (52°C for 30 s), and elongation (72°C for 90 s). Reactions ended with a final elongation step (72°C for 7 min). The minireplicon fragments tested were amplified with primers str7 5′-CGCAGAT AAGCCAGCGCATC-3′ (coordinates 44251 to 44270) and 6L2 5′-AAGCGGG TAGTGATAGACTG-3′ (coordinates 1497 to 1478), str7 and inp5 5′-AGTGA TTCCGTACGGGGCCA-3′ (coordinates 45512 to 45493), str7 and rep2, and miniR1 5′-GC*GGATCC*GCGTTGCGTAGTCGTCTAG-3′ (coordinates 45693 to 45711) and snab2 5′-CG*GCATGC*CGATCACGCTCCCAGGTCAA-3′ (coordinates 2347 to 2329). PCRs were performed as described above with an annealing temperature of 54°C and an elongation time of 3 min in each cycle. All PCR-derived clones were analyzed by DNA sequencing to check their fidelity.

Plasmid DNA isolation, analysis, cloning, and manipulation. Plasmid RA3 DNA was extracted with a midi kit used according to the manufacturer's instructions (Qiagen, West Sussex, United Kingdom). Plasmid DNA was isolated and manipulated by standard procedures (29). For the cloning of PCR fragments, either promoter-probe vector pPTO1 (39) or expression vector pGBT30 (17) with *lacI*^{q} and *tacp* was used. The plasmids used and constructed in this study are presented in Table 1.

Sequencing and sequence assembly. Sequencing reactions were performed with custom primers with RA3 as the template. A library of EcoRI fragments of RA3 was created in pUC18, and partially HincII-digested DNA was also inserted into pUC18 to assist the sequencing of problematic regions with the use of universal primers. Sequences were generated with the ABI Big Dye terminator kit. Sequences were assembled with the DNASTAR Lasergene 99 package. Restriction enzyme analysis verified the assembly. Open reading frame (ORF) predictions were made with Glimmer 2.0 according to standard parameters. The function of each ORF was predicted by BLAST searches against the EMBL/SWISSPROT databases, and the function was annotated based on homology. The predicted proteins were characterized by isoelectric point and molecular weight and searched for coiled-coil regions, conserved domains, and transmembrane helices with the use of bioinformatics on-line software on the EXPASY

server (pI, MolMass, Coils, InteroScan [EMBL-EBI], and TMHMM v2.0 [CBS], respectively).

Determination of catechol 2,3-oxygenase activity (XylE). Catechol 2,3-oxygenase activity (the product of *xylE*) was assayed (44) in exponentially growing bacteria. Plasmid content of all assayed cultures was monitored to ensure that differences in XylE activity were not due to variations in plasmid copy number. One unit of catechol 2,3-oxygenase is defined as the amount needed to convert 1 μmol of catechol in 1 min under standard conditions. Protein concentration was determined by the Bradford method (5).

Transformation and conjugation procedures. *E. coli* competent cells were prepared by $CaCl_2$ treatment (29). Samples (0.2 ml) of overnight cultures of the donor and recipient strains grown under selection were pelleted at 5,000 × *g* for 2 min, and the pellets were resuspended in 100 μl of fresh medium. Recipient and donor cell suspensions were mixed (2:1), spread on L agar, and incubated overnight at 37°C (for *E. coli*) or 28°C (for *P. putida*, *R. eutropha*, and *A. tumefaciens*). Cells were suspended in 1 ml of L broth. Cell suspensions were serially diluted, plated on L agar with appropriate selection, and allowed to grow for 48 h.

***oriT* mapping.** A restriction fragment of 458 bp (coordinates 9397 to 9854) predicted to contain *oriT* was cloned into pAKE600 to create pAKB9.5. *E. coli* DH5α harboring RA3 was transformed with pAKE600 or pAKB9.5. The double transformants were used as donors in conjugal-transfer mating experiments with *E. coli* K-12 strain CV601 as the recipient, with selection for either Pn^r Kn^r (pAKE600) or Cm^r Kn^r (RA3) transconjugants. Transconjugants were then tested for the presence of the mobilized or conjugative plasmids (DNA analysis).

Stability assays. *E. coli*, *A. tumefaciens*, *R. eutropha*, and *P. putida* harboring RA3 were grown overnight in liquid cultures with selective pressure and analyzed for plasmid content. The cultures were then diluted 10^5-fold and grown without selection over 20 generations, and dilutions were plated onto L agar plates with and without chloramphenicol to estimate plasmid retention. The procedure was repeated over 60 generations. Plasmid content was also checked at the end of the experiment.

Nucleotide sequence accession number. The annotated sequence of plasmid RA3 has been deposited in the GenBank database under accession number DQ401103.

RESULTS AND DISCUSSION

RA3 host range. Conjugative plasmid RA3 was originally isolated from *Aeromonas hydrophila* and was also stably maintained in *E. coli* (3). The host range of RA3 was examined by conjugal-transfer mating experiments. RA3 was transferable to a wide spectrum of gram-negative bacteria, among them *P. putida* (gammaproteobacteria), *R. eutropha* (betaproteobacteria), and *A. tumefaciens* (alphaproteobacteria). The frequency of transfer between *E. coli* and either *P. putida* or *R. eutropha* was very high (1×10^{-1} transconjugant per donor). The frequency of transfer between *E. coli* and *A. tumefaciens* was much lower (1×10^{-4} transconjugant per donor under the conditions tested). RA3 retention in populations of transconjugants of *A. tumefaciens*, *R. eutropha*, and *P. putida* was evaluated every 20 generations during growth without selection for approximately 60 generations. RA3 replicated and was stably maintained in almost 100% of the cells after 60 generations of nonselective growth in all three subgroups of proteobacteria. The restriction enzyme profiles of plasmid DNA isolated from transconjugants at the end of the stability experiments were similar to the profiles of the original plasmid indicating that these were not chromosomal integrants (data not shown).

General features of RA3. The 45,909-bp sequence of plasmid RA3 was determined by primer walking; when necessary, subcloned restriction fragments were sequenced with universal primers.

The number of identified coding sequences within the RA3 plasmid is 50, based on a Glimmer 2.0 cutoff of 250 bp, followed by visual inspection. Among the 50 ORFs, only 1 (*orf11*) has no homologs in public databases and 10 have homologs of unknown function (Table 2; for the full version, see Table S1 in the supplemental material). Forty-four of the ORFs show 100% identity to ORFs found in pFBAOT6 from the IncU incompatibility group (accession no. NC_006143; 27). Hence, the annotation of RA3 arbitrarily follows that for pFBAOT6 in the region from the first base pair to 33 kb, with the exception of *orf01*, which is designated *repB* instead of *rep*. The equivalent of *orf50* (coordinates 45441 to 45737) has not been identified in the pFBAOT6 annotation, but there is strong experimental evidence that this locus is a part of the replication cassette (see below) and was thus annotated in RA3 as *repA*.

Plasmid RA3 has an uneven distribution of restriction endonuclease recognition sites (Fig. 1A and B). The backbone region seems to be inaccessible to most of the common restriction endonucleases, with the exception of EcoRI; 11 GAATTC palindromic sequences are found in the region coding for replication and conjugative-transfer functions. This observation was made previously with IncU plasmid pRAS1 (35) and may indicate that *E. coli* is a relatively new host for RA3. Aside from EcoRI, the majority of sites sensitive to digestion by class II restriction enzymes localize to the integron (coordinates 34138 to 43493), suggesting recent acquisition of this DNA.

The average GC content of the RA3 sequence is 53.6% (10). For comparison, two recently sequenced chromosomes of *A. salmonicida* subsp. *salmonicida* (NC_009348) and *A. hydrophila* subsp. *hydrophila* (NC_008570) show higher GC contents of 58% and 61%, respectively. The GC content of RA3 varies along the plasmid molecule (Fig. 1C), and the fluctuations coincide with the boundaries of functional modules, with a minimum value of 33% around position 37,000 bp (integron) and the maximum reaching 68% at position 8,500 bp in the stability region.

RA3 contains long repetitive sequences that are also evident in some broad-host-range environmental plasmids, e.g., pIPO2 (37) and pSB102 (34). The repetitive sequences in RA3 fall into two categories: intragenic repetitions translated into protein domains (class I) and intergenic long repetitive sequences (class II). Both repetitions show considerable sequence conservation that ranges from 85 to 100% for a particular unit. Moreover, a characteristic feature of these sequences is their compact structure; the units are organized head to tail, forming a repeat module.

The class I repetitions were found in three loci (Fig. 2), *orf07*, *orf10*, and *orf17*, which code for proteins KfrA, KorB, and TraC4, respectively. The lengths of the repeated units vary from 13 amino acids in TraC4 to 19 amino acids in KorB and 35 amino acids in KfrA. The class II repetitions of 345 and 537 bp surround the replication module and are described in detail below.

Modular structure and transcriptional organization. Genes in the plasmid backbone (coordinates 45019 to 31194) are organized in blocks associated with particular functions such as replication, stable maintenance, and conjugative transfer (Fig. 2). These three functional modules seem to be of distinct origins showing homology to unrelated groups of plasmids. The genetic organization of the RA3 backbone reveals a compact structure (Fig. 2). The coding sequences cover 91% of the RA3 backbone and 96% of the plasmid when the two long repetitive regions surrounding the *rep* genes and the intergenic

TABLE 2. Predicted coding sequences in RA3

ORF	Gene	Coordinates[a]	Size in aa (mass in kDa)	% Similarity, homolog (protein ID)	pFBAOT6 (protein ID)
01	*repB*	1–1380	459 (52.27)	82, $RepA_{Rms149}$ (CAI46990)	CAG15048
02	RA3.02	2248–2526	92 (11.41)		CAG15049
03	*klcA*	2637–3062	141 (16.35)	55, $KlcA_{R751}$ (NP044227)	CAG15050
04	RA3.04	3190–3345	51 (5.71)		CAG15051
05	*korC*	3391–3687	98 (10.84)	55, $KorC_{RK2}$ (C35387)	CAG15052
06	*kfrC*	3692–4759	355 (38.57)	69, $KfrC_{R751}$ (Upf54.4) (AAC64416)	CAG15053
07	*kfrA*	4889–5956	355 (38.68)	30, $KfrA_{R751}$ (AAC64418)	CAG15054
08	*korA*	6037–6348	104 (11.3)	53, $KorA_{RK2}$ (P03052)	CAG15055
09	*incC*	6353–7105	250 (27.11)	63, $IncC_{RK2}$ (P07673)	CAG15056
10	*korB*	7102–8460	452 (47.81)	53, $KorB_{RK2}$ (P07674)	CAG15057
11	RA3.11	8463–8690	75 (7.93)		Not annotated
12	*mpR*	8816–9547c	243 (27.3)	61, MpR_{R46} (AAD17385)	CAG15059
13	*mobC*	9837–10367	176 (19.97)	57, $MobA_{pXF51}$ (AAF85616)	CAG15060
14	*nic*	10360–11355	331 (36.9)	63, $MobB_{pXF51}$ (AAF85615)	CAG15061
15	*traC3*	11394–13088c	564 (62.19)	59, $TraC2_{R751}$ (AAC64468)	CAG15062
16	*traD*	13091–13237c	48 (5.3)	60, $TraD_{R751}$ (AAC64471)	CAG15063
17	*traC4*	13227–16292c	1021 (111.9)	51, $TraC4_{R751}$ (AAC64469)	CAG15064
18	*virD4*	16305–18230c	641 (72)	55, $TraN_{pIPO2}$ (CAC82760)	CAG15065
19	*virB11*	18196–19188c	330 (37.3)	66, $VirB11_{pAT}$ (AAL45862)	CAG15066
20	*virB10*	19202–20416c	404 (42.3)	55, $TraL_{pIPO2}$ (CAC82758)	CAG15067
21	*virB9*	20416–21249c	277 (30.54)	63, $VirB9_{pXF51}$ (AAF85582)	CAG15068
22	*virB8*	21252–22001c	249 (28.1)	61, $VirB8_{pXF51}$ (AAF85581)	CAG15069
23	RA3.23	22001–22207c	68 (7.4)	51, OPRF from *Brucella melitensis* 16M (AAL53277)	CAG15070
24	*virB6*	22322–23332c	336 (35.4)	54, $VirB6_{pXF51}$ (AAF85580)	CAG15071
25	RA3.25	23344–23613c	89 (9.73)	65, $TraG_{pIPO2}$ (CAC82753)	CAG15072
26	*virB5*	23648–24292c	214 (23.44)	53, $TraF_{pIPO2}$ (CAC82752)	From 24286 identical to CAG15073
27	*virB4*	24289–26736c	815 (91.70)	68, $VirB4_{pXF51}$ (AAF85576)	CAG15074
28	*virB3*	26733–27053c	106 (11.90)	61, $VirB3_{pXF51}$ (AAF85575)	CAG15075
29	*virB2*	27071–27394c	107 (11.21)	54, $VirB2_{pXF51}$ (AAF85574)	CAG15076
30	RA3.30	27372–27728c	118 (13.6)	67, XF_a0004_{pXF51} (AAF85573) from *Xylella fastidiosa* 9a5c	CAG15077
31	*top*	27793–29769c	658 (72.29)	73, $TopA_{pXF51}$ (AAF85572)	CAG15078
32	RA3.32	29766–30503c	245 (26.23)	45, LysM from *Desulfotomaculum reducens* MI-1 (EAR43569)	CAG15079
33	RA3.33	30514–31008c	164 (17.97)	56, TraL from *Dichelobacter nodosus* (AAW31839)	CAG15081
34	RA3.34	31194–31583	129 (14.06)		CAG15082
35	RA3.35	31603–31863	86 (9.52)	71, Ypesb_01003249 from *Yersinia pestis* (ZP_01175336)	CAG15083
36	RA3.36	31856–32251	131 (14.89)	44, Nham_0207 from *Nitrobacter hamburgensis* X14 (ABE61107)	CAG15084
37	*rec*	32316–32885c	189 (20.89)	79, $PinR_{pMAQU01}$ from *Marinobacter aquaeolei* VT8 (ABM21007)	CAG15085
38	*tnp*	33177–33971c	264 (30.71)	100, Tnp_{pRAS1} (CAD57187)	CAG15086
39	*orf6*	34138–34425c	95 (9.77)	100, $Orf6_{pRAS1}$ (CAD57186)	CAG15087
40	*orf5*	34449–34949c	166 (18.33)	99, $Orf5_{pRAS1}$ (CAD57185)	CAG15088
41	*sulI*	35076–35915c	279 (30.12)	100, $SulI_{pAr-32}$ (CAD57201)	CAG15089
42	*qacEdelta1*	35909–36115c	68 (7.42)	97, truncated $QacEdelta1_{pAr-32}$ (CAD57200)	
43	*catA2*	36861–37502c	213 (24.77)	99, $CatA2_{pAr-32}$ (CAD57199)	
44	*tnp513*	38253–39794c	513 (58.49)	100, Tnp_{pAr-32} (CAD57198)	
45	*sulI*	40199–41038c	279 (30.12)	100, $SulI_{pAr-32}$ (CAD57201)	
46	*qacEdelta1*	41032–41379c	115 (12.33)	100, $QacEdelta1_{pAr-32}$ (CAD57196)	CAG15090
47	*aadA2*	41543–42334c	263 (29.54)	100, $AadA2_{pY2}$ from *Klebsiella pneumoniae* (AAF87686)	CAG15091
48	*int1*	42480–43493	337 (38.38)	100, $IntI_{pRAS1}$ (CAD57181)	CAG15092
49	*res*	43836–44411c	191 (20.28)	100 (in 174 aa), $Pin_{pRSB101}$ (CAG27808)	CAG15093[b]
50	*repA*	45441–45737	98 (10.91)	58, VapI from *Rhodopseudomonas palustris* BisB18 (YP_531137); 54, $HigA_{Rts1}$ (AAC43983)	Not annotated

[a] The letter c follows the coordinates of ORFs on the complementary strand. The hypothetical presence of transmembrane helices within the predicted proteins was analyzed with TMHMM v 2.0 software.
[b] 93% homology.

region between maintenance and transfer modules encoding *oriT* (see below) (1,400 bp) are subtracted. The region of RA3 encompassing the integron (coordinates 31194 to 45019) shows only 72% coding sequences.

There are 17 predicted promoters in the RA3 sequence. Twelve of the promoters potentially drive the expression of the majority of backbone functions, with nine oriented clockwise and three counterclockwise (Table 3 and Fig. 2). There are three

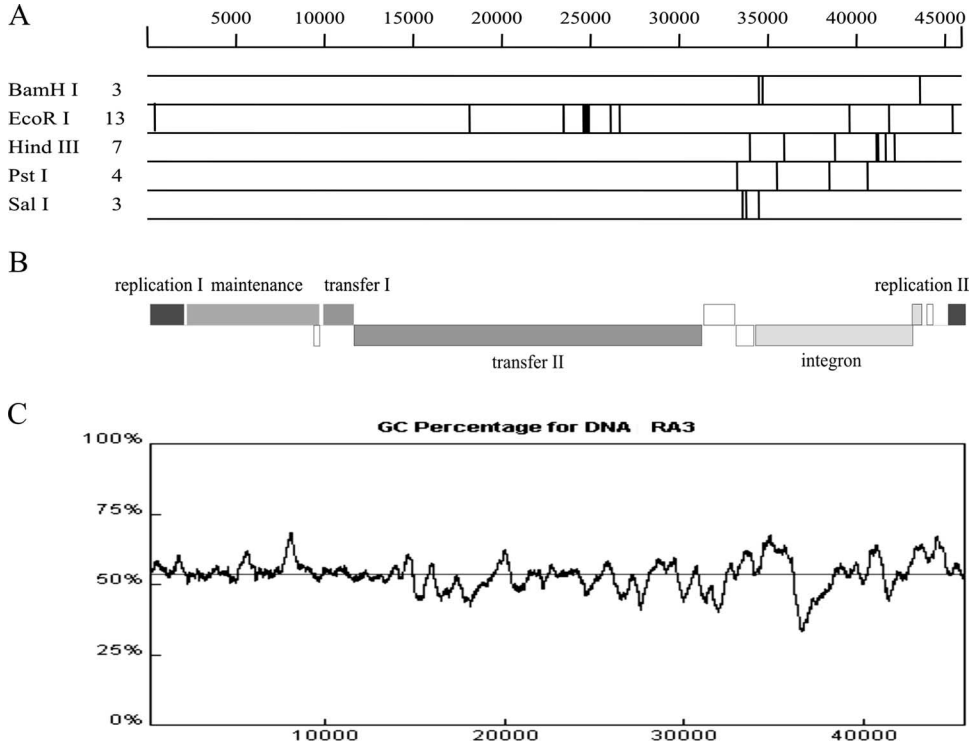

FIG. 1. RA3 sequence analysis. (A) Restriction map of the RA3 sequence generated in silico. The map shown (Lasergene package) represents RA3 restriction patterns for BamHI, EcoRI, HindIII, PstI, and SalI. The number of recognition sequences is indicated at the left. (B) Modular organization of RA3 with plus- and minus-strand genes. (C) GC content of the RA3 DNA sequence. The *x* axis indicates the plasmid sequence coordinates, while the *y* axis shows the percentage of GC counted for a 500-bp window.

putative divergent promoter regions: *repBp*/*repXp* within the replication module, *mpRp*/*mobCp* between the maintenance and conjugative transfer-associated genes, and RA3.33*p*/RA3.34*p* in the conjugative transfer region.

Replication functions. The predicted replication region of RA3 spans >3 kb (coordinates 45019 to 2069) and encompasses two ORFs, designated *repA* and *repB* (Fig. 3B). As repetitive sequences upstream and downstream of the *repAB* genes are homologous, the arbitrarily identified separate units building both regions were designated r1 (38 bp), r2 (42 bp), and r3 (60 bp) (Fig. 3C) to differentiate between sequences that are common or distinct in these two regions. The final 11 nucleotides (nt) are conserved in all three units (in italics in Fig. 3C). The repetitive sequences (346 bp) upstream of *repA* (designated r1/r3) are organized as $(r3r1)_3r3$. The repetitions (557 bp) located downstream of *repB* (designated r1/r2) are organized as $(r1r2)_3r1(r1r2)_3r1$. Interestingly, 25 bp of the r3 unit is present within the 3′ terminus of the *repB* coding sequence (Fig. 3B; underlined in panel C).

RA3 replication is independent of polymerase I, as shown by propagation in the *polA* mutant *E. coli* C2110. To examine the minimal requirements for replication activity, PCR fragments corresponding to different parts of the replication region (Fig. 3B) were cloned into the pGEM-T Easy vector and tested for the ability to replicate in the C2110 strain, which is not transformable by pGEM-T Easy alone. A fragment encompassing *repB* with the r1/r2 repetitive region (coordinates 45693 to 2248) was sufficient for replication (pMOB1.4; Fig. 3B). Neither *repA* nor the upstream repetitive region r1/r3 was required for minireplicon functionality. A fragment containing *repB* without the r1/r2 repetitive region was incapable of transforming the C2110 strain (pAKB1.101), suggesting that the isolated r3 unit in the 3′ end of *repB* is insufficient for *oriV* activity. The AT percentage plot for the RA3 replication region (coordinates 44251 to 2248) revealed the existence of several AT-rich stretches, with two (>60% AT) within the minimal replicon (Fig. 3A and B). The first of these regions is located between the end of *repB* and the downstream r1/r2, and the second AT-rich stretch is immediately after the r1/r2 boxes. The RA3 sequence was also inspected for the presence of the highly conserved DnaA box sequence ($5'TT^A/_TTNCACA$) (32), but no motifs were identified. This may suggest that the DnaA initiator protein is not necessary for replication initiation in RA3.

Plasmid-encoded toxins-antitoxins eliminate plasmid-free cells that emerge due to segregation or replication defects. Chromosomal homologs of toxin-antitoxin genes are widely distributed in bacteria and induce programmed cell death or reversible cell cycle arrest in response to starvation or other adverse conditions (14). The predicted RepA protein is a polypeptide of 98 amino acids (10.91 kDa) that shows 34% identity to the HigA antitoxin from plasmid Rts1 of *Proteus vulgaris* (40) (Fig. 4). Similarly, RepA is homologous to a number of chromosomally encoded antidote proteins from alphaproteobacteria that are characterized by a VapI-like domain: the protein shares 41 to 44% identity with putative antitoxins from *Mesorhizobium loti*, *Sinorhizobium meliloti*, and *Rhodospirillum rubrum*. No obvious candidate for a toxin gene

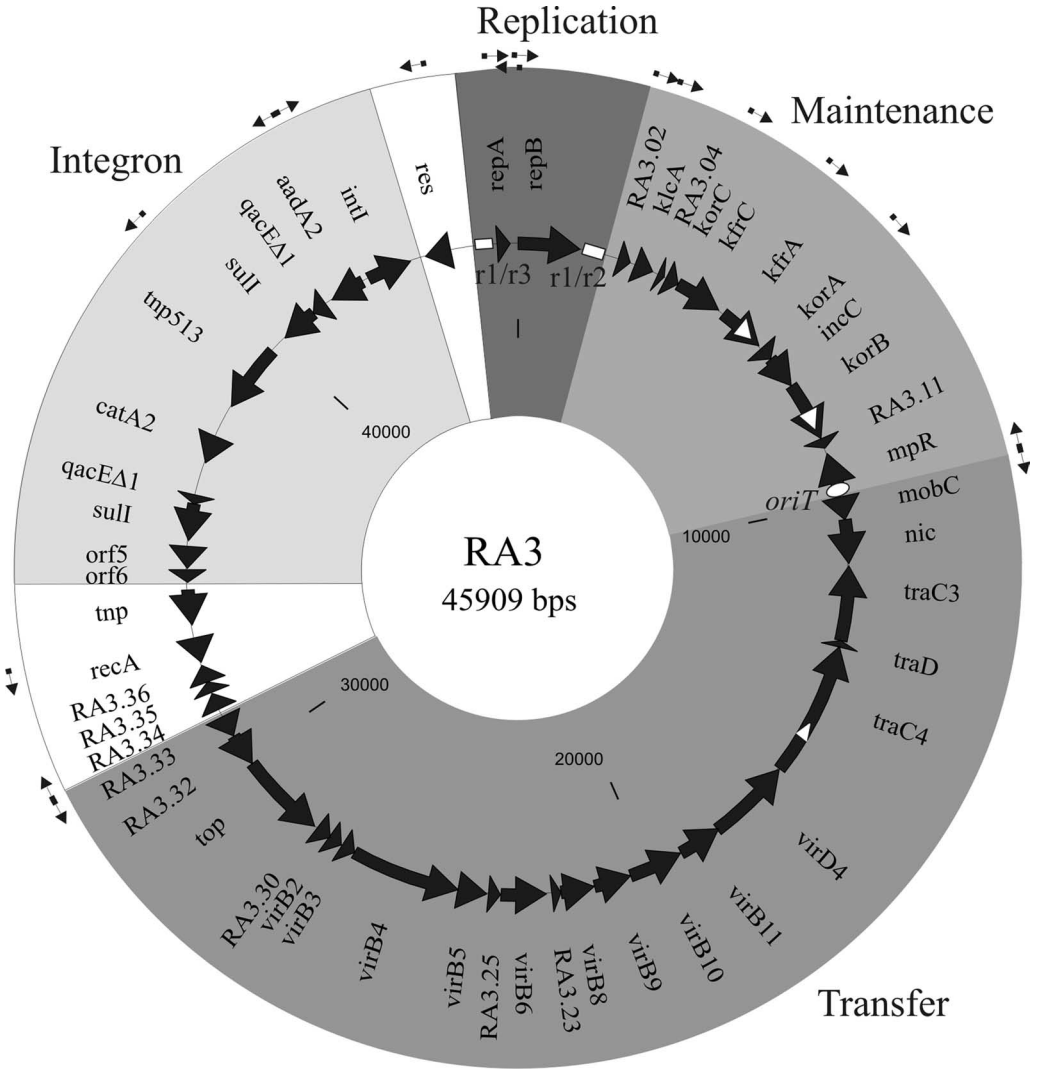

FIG. 2. Circular representation of plasmid RA3. All identified ORFs are represented by solid arrows indicating the direction of transcription. Functional gene clusters are highlighted with different shades of grey. The genes which are not obvious parts of the modules are left white. The predicted promoters are marked with thin black arrows. The class I intragenic repetitions in *kfrA*, *korB*, and *traC* and the class II repetitive regions r1/r3 and r1/r2 are represented by white triangles and boxes, respectively. The white oval marks the position of *oriT*.

TABLE 3. Predicted promoters in the RA3 sequence[a]

Locus	−35 motif (coordinates)	Spacer size (bp)	−10 motif (coordinates)
repB	TTGGCG (45762–45767)	17	TAAATT (45785–45790)
RA3.02	TTGCCA (2168–2173)	18	TATAAT (2192–2197)
klcA	TTGACA (2558–2563)	18	TATTAT (2582–2587)
korC	TTGAGG (3175–3180)	20	TATTGT (3201–3206)
kfrA	TTGTAT (4829–4834)	18	TAAAAT (4853–4858)
korA	TTGACG (5967–5972)	16	TATCTT (5989–5994)
mpR	TGGCTC (9641–9646c)	12	TAACTT (9623–9628c)
mobC	TTGCTA (9761–9766)	16	TAAAAT (9787–9792)
RA3.33	TGTCCA (31079–31084c)	17	TATATT (31056–31061c)
RA3.34	TGGCCT (31136–31141)	18	TACCAT (31160–31165)
rec	TCCCCG (32958–32964c)	18	TAAAAT (32935–32940c)
tnp513	CTGATA (39994–39999c)	16	TATTGT (39972–39977c)
aadA2	TGGACA (42590–42595c)	17	TAAACT (42567–42572c)
int1	TTGCTG (42425–42430)	17	TAGACT (42448–42453)
res	TTGCGC (44457–44472c)	17	TAAGAT (44444–44449c)
repA	TTGTTG (45379–45384)	17	TACACT (45402–45407)
repX	TTGCCA (45886–45891c)	16	TATAAT (45864–45869c)

[a] The putative −35 and −10 motifs are accompanied by the sequence coordinates in plasmid RA3 (DQ401103). The letter c follows the coordinates of promoters on the complementary strand.

is evident in RA3. Protein structure predictions for RepA revealed the existence of a Cro/cI-type DNA-binding domain (residues 15 to 68) present in the XRE family of transcriptional regulators with an α-helix–turn–α-helix (HTH) motif spanning residues 25 to 42 (Fig. 4), and regulatory studies (see below) confirmed its role in the repression of *repAp*.

The putative RA3 replication initiation protein RepB (459 amino acids, 52.27 kDa) is encoded downstream of *repA*. RepB shows >99% identity with the putative replication protein of IncU plasmid pFBAOT6: the proline at position 450 of RepB is changed to alanine in the pFBAOT6 homolog. RepB is 70% identical and 82% similar to RepA from Rms149. RepB of RA3 also shows high levels of similarity (69 to 81%) to putative replication initiation proteins of plasmids isolated from species belonging to alpha-, beta-, and gammaproteobacteria (Fig. 5). Intriguingly, RepB also has lower, but significant, similarity to putative replication proteins from plasmids of gram-positive

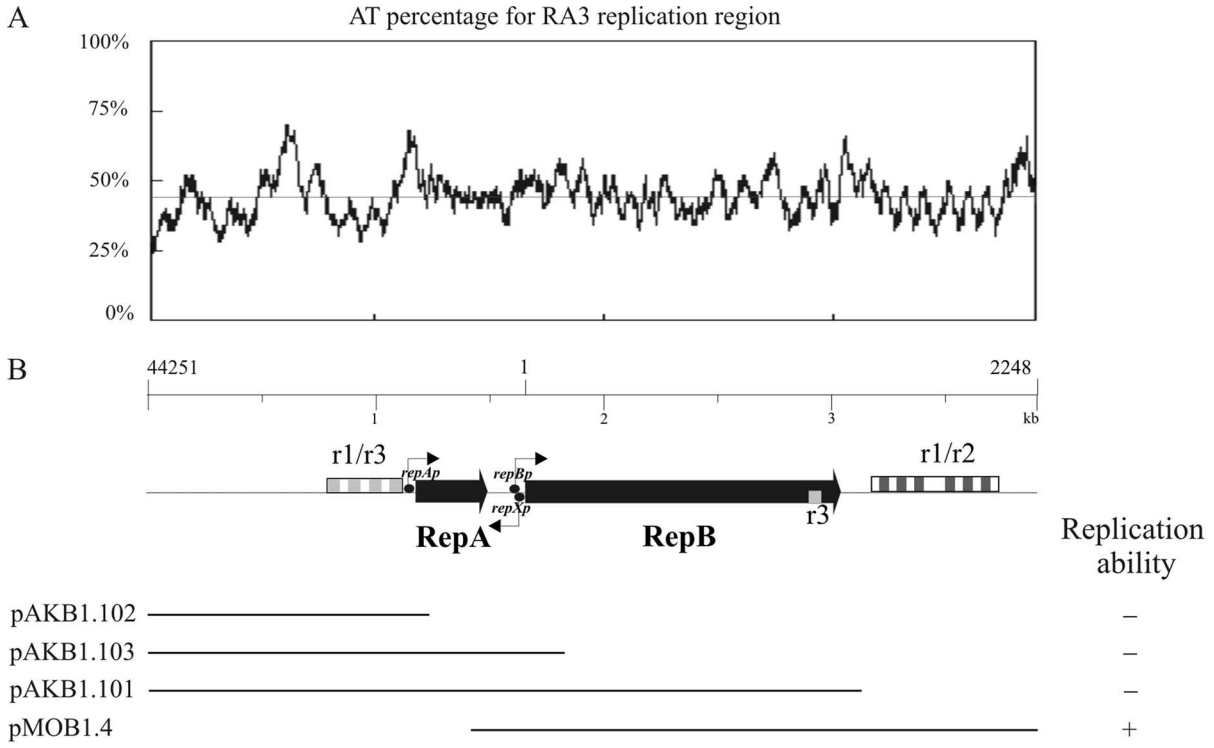

C

r1 GCCAACTCACCAGGCACCGGCAGCAGC*TCAACCAGGTG*
r2 GCCAAGTTCAGATCTGGACGCCAGAAGGAAA*TCAACCAGGTG*
r3 ATCGCCTCGATGCGGTGAGACAAGTCCCTCCCCTATTACAGGCGGCAGC*TC*G*ACCAGGTG*

FIG. 3. Replication region of RA3. (A) AT percentage plot for the region from 44251 to 2248 encompassing the replication module. The *x* axis indicates the position in the RA3 sequence. (B) Functional mapping of the replication region. The organization of the replication module is depicted with thin black arrows marking the putative transcription start points, black circles marking putative promoters, and combinations of the repetitive sequences indicated by boxes as follows: r1, white; r2, dark grey; r3, light grey. The bottom part of the panel illustrates the DNA fragments cloned into a high-copy-number vector (pMB1 origin) and tested for the ability to replicate in *E. coli* C2110 (*polA*). The results of the tests are summarized on the right. (C) Repetition units r1, r2, and r3. The sequence that is the same in all three units is in italics; the fragment of repetition unit r3 found at the 3′ end of $repB_{RA3}$ is underlined.

bacteria, i.e., 47% and 50% similarity to Rep43 of *Bacillus* sp. strain KSM-KP43 plasmid (28) and to Rep of pIP404 from *Clostridium perfringens* (8), respectively. The conservation in the RepB homologs is sustained over the N-terminal 380 amino acids, whereas the C termini of the polypeptides are variable (Fig. 5). The predicted HTH motif in RepB is positioned in the C-terminal domain between residues 406 and 427, so the recognition specificity for the replication origins apparently is determined by the most variable protein segment.

As described above, the 3′ end of *repB* of RA3 includes a partial r3 repetition, a variant of which is present in two copies in the putative replication gene of Rms149, where it was proposed to act as an origin of replication (12). Interestingly, Rms149 does not possess the extended r1/r2 and r1/r3 repetitive sequences found in RA3. A homologous part of the r3 motif also is present in two copies in pKBB4037, one in a position at the 3′ end of *rep*, similar to that in RA3 and Rms149, and a second located intergenically downstream of *rep*. Plasmid2 from *Nitrosomonas eutropha* C91 also possesses a partial r3 repeat located downstream of its putative replication gene. As the r3 motif seems to have different roles in Rms149 and RA3, it would be interesting to ascertain the incompatibility types of these sequenced plasmids, along with their host ranges, building on the initial functional minireplicon analysis performed with RA3 (see above), Rms149 (12), and pRSB105 (33). Rms149 has been classified into the IncP-6 group of *Pseudomonas* plasmids and IncU (IncG) groups of *E. coli* plasmids (12); however, the host range of Rms149 has not been fully examined. The pRSB105 plasmid encodes two functional replication systems, one with a narrow host range which is active in several gammaproteobacteria and a second homologous to Rms149 which is also active in gammaproteobacteria and which extends the plasmid's host range to betaproteobacteria but not to alphaproteobacteria. The host range of RA3 seems to be the broadest among the three plasmids because, as noted above, it can replicate and be stably maintained in alpha-, beta-, and gammaproteobacteria.

To further understand the function of the *rep* locus in RA3, a transcriptional analysis of this region was initiated. Putative promoters were found in silico in the replication module pre-

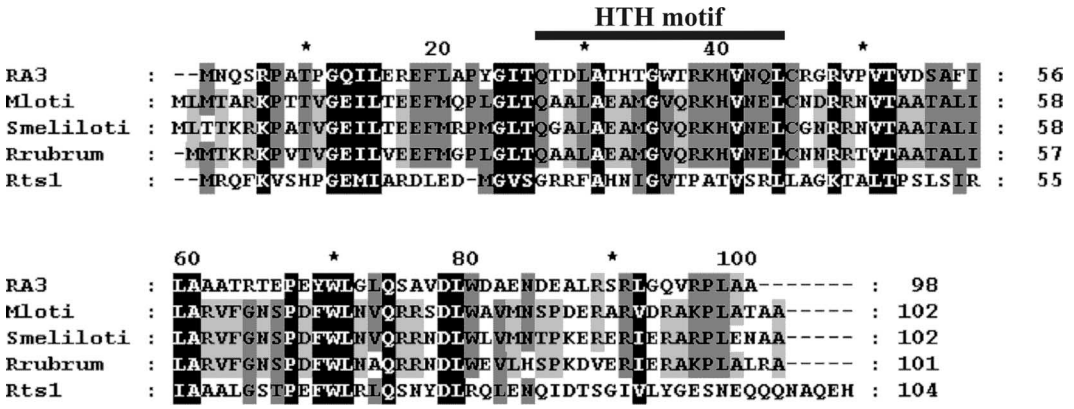

FIG. 4. Amino acid sequence conservation of $RepA_{RA3}$ (ABD64877) and homologous antidote proteins in *M. loti* MAFF303099 (BAB48919), *S. meliloti* strain 1021 (CAC45622), *R. rubrum* (YP_426153), and plasmid Rts1 of *P. vulgaris* HigA (AAC43983) (the GenBank/EMBL database protein accession numbers are given in parentheses). Identical or functionally similar residues in the five sequences are shown with a black background, and those that are conserved in three or four representatives are shown with two shades of grey background. The HTH motif identified in $RepA_{RA3}$ (residues 25 to 42) is indicated.

ceding the *repA* and *repB* coding sequences (Table 3), and an additional promoter, *repXp*, is evident on the complementary strand in the *repA-repB* intergenic region (see Fig. S1 in the supplemental material). The region between the end of the upstream repetitive module and the *repA* start covers 77 bp (coordinates 45364 to 45441) and includes *repAp* and two imperfect inverted repeats (IRs) with 12- and 7-bp arms that may have a potential regulatory role. The region immediately upstream of *repB* includes two putative promoter sequences designated *repBp1* and *repBp2* and divergently oriented *repXp*, which overlaps *repBp2*. Fragments bearing these putative promoters were PCR amplified and cloned into promoter-probe vector pPT01 upstream of a promoterless *xylE* cassette (39). The relative transcriptional activities of the analyzed regions were assessed by measuring levels of catechol oxygenase XylE expressed from the transcriptional fusions (Fig. 6). The *repAp* promoter upstream of *repA* showed moderate transcriptional activity (pMOB1.10.1; 0.2 U of XylE). No promoter activity was detected for *repBp2* (pMOB1.8.1), whereas a fragment containing both *repBp1* and *repBp2* showed low transcriptional activity (pMOB1.7.1; 0.01 U of XylE). This activity seems to be sufficient for the expression of *repB* in the minireplicon tested in the *polA* mutant (pMOB1.4), although the possibility cannot be excluded that readthrough transcription from a vector promoter might fortuitously drive *repB*. Transcription from *repBp1* is expected to produce a 113-nt 5′ untranslated region that may be highly structured since it includes a long imperfect IR spanning 46 bp (see Fig. S1 in the supplemental material).

The strongest promoter in the *rep* region is *repXp*, which generates 0.5 U of XylE activity in a transcriptional fusion with the promoterless *xylE* cassette (pMOB1.9.1; Fig. 6). The *repXp* promoter either may be responsible for the synthesis of an antisense regulatory RNA that could interact with *repB* mRNA over a 71-nt stretch or may direct the expression of the ORF encoding a putative RepX polypeptide of 38 amino acids. The start codon of this ORF overlaps the stop codon for *repA* (see Fig. S1 in the supplemental material). Thus, RepX may be a part of a regulatory circuit that controls RA3 replication. Additionally, the *repXp* promoter may also influence the activity of the overlapping *repBp* promoter by competing for binding of RNA polymerase in this region. Further studies are currently under way to distinguish between these possibilities.

The *repA* and *repB* genes were PCR amplified and cloned under control of the inducible *tacp* promoter in expression vector pGBT30 (17) to generate pMOB1.5.1 and pMOB1.6.1, respectively. The expression plasmids were introduced into C600K cells carrying the *repAp-xylE* (pMOB1.10.1), *repBp-xylE* (pMOB1.7.1), or *repXp-xylE* (pMOB1.9.1) transcriptional fusion. Double transformants were grown in the presence of IPTG to induce the synthesis of RepA or RepB to allow an assessment of whether either protein regulates expression from any of the three promoters. Both RepA and RepB downregulated the expression of *repAp* 5- to 10-fold (Fig. 6). Further studies are required to assign the operator sites for the two regulators, although it is interesting that there are two IR motifs in the *repAp* region that are candidate sites for RepA and/or RepB interaction. By contrast, neither *repBp* nor *repXp* was sensitive to the presence of excess RepA or RepB (Fig. 6). Nevertheless, the divergent promoter region that includes the *repBp2* and *repXp* promoters contains a 46-bp imperfect IR that overlaps both promoters (see Fig. S1 in the supplemental material).

Maintenance functions. The ORFs related to maintenance functions in RA3 are clustered in a region of 7.7 kb (coordinates 2069 to 9836) located downstream of *repB*. The region contains 10 ORFs transcribed/translated in the clockwise direction and one oriented in the counterclockwise direction (Fig. 7A). The seven ORFs that are most closely related to IncP-1 counterparts (25, 38) were designated *klcA*, *korC*, *kfrC*, *kfrA*, *korA*, *incC*, and *korB*. Their products are predicted (on the basis of homology) to form a partitioning apparatus, provide regulatory circuits, and act as accessory stabilization factors. The transcriptional organization of this region suggests that there are promoter regions upstream of five of the genes, *orf02*, *klcA*, *korC*, *kfrA*, and *korA*. The putative partitioning operon of RA3 consists of four ORFs, *korA*, *incC*, *korB*, and *orf11*, with IncC (63% identical to $IncC2_{RK2}$) belonging to the ParA family of Walker-type ATPases (19) and KorB (53%

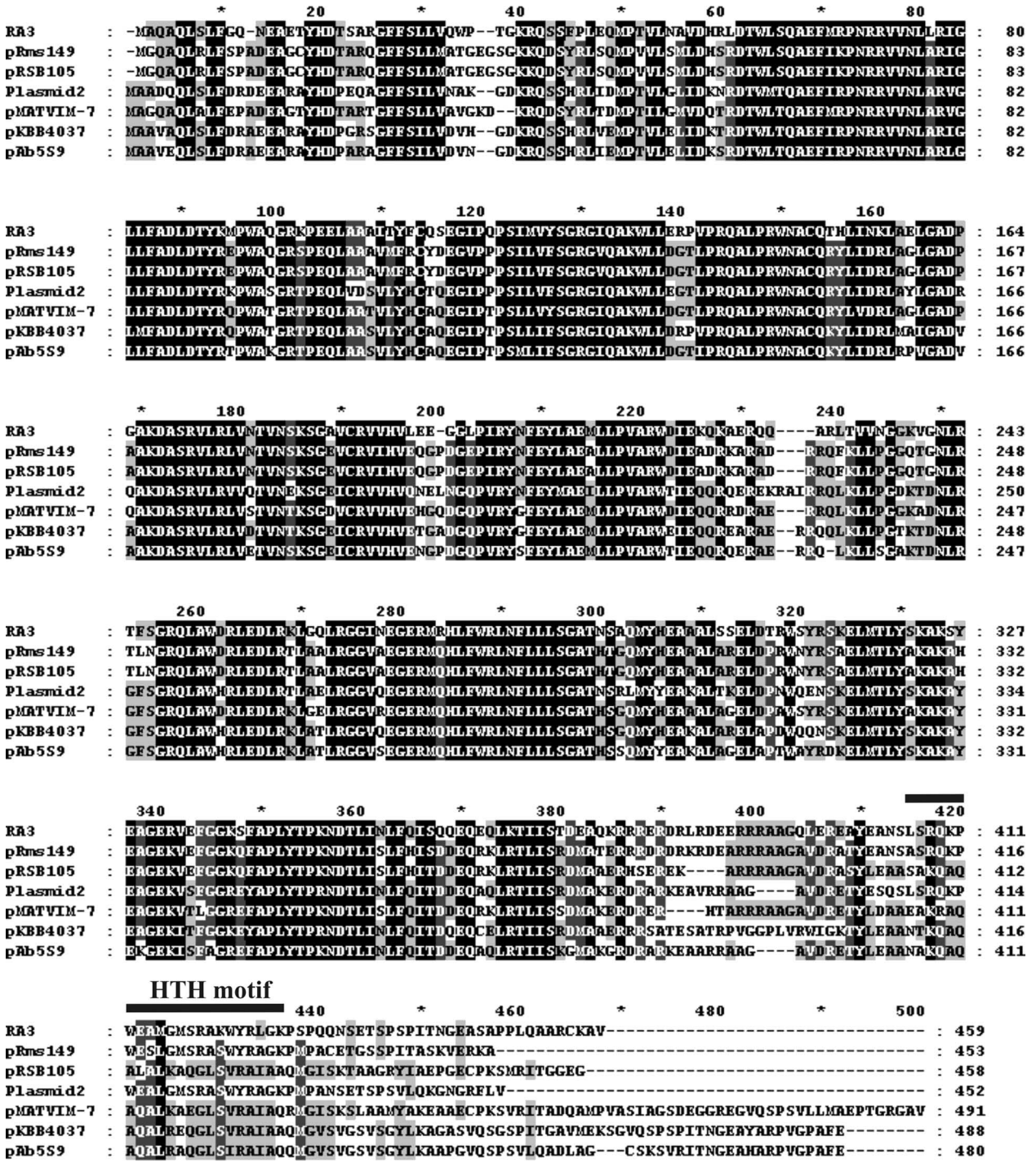

FIG. 5. Sequence alignment of the $RepB_{RA3}$ and homologous replication initiation proteins. Conserved residues in replication initiation proteins from RA3 (ABD64829), Rms149 (YP_245484), pRSB105 (ABI20460), pAb5S9 (YP_001220601), pMATVIM-7 (YP_001427363), pKBB4037 (CAI47016), and Plasmid2 (YP_743798) (GenBank/EMBL database protein accession numbers are given in parentheses) are shown by a black background. Residues identical or functionally similar in five polypeptides are marked with a dark grey background, and residues conserved in four representatives are shown with a light grey background. The predicted HTH motif in the RepB polypeptide of RA3 is indicated.

identical to $KorB_{RK2}$) acting as the ParB DNA-binding homolog. Unusually among KorB/ParB homologs, KorB of RA3 possesses a class I repetitive sequence in the linker region between the N and C domains. ORF11 has been annotated in the pFBAOT6 sequence, but in a different reading frame. The RA3 partition operon is autoregulated by KorA (A. Kulinska and G. Jagura-Burdzy, unpublished data). Interestingly, the putative partitioning operons of the pIPO2 and pSB102 plasmids from bacteria of the wheat and alfalfa rhizospheres (34, 37) consist of *korA-incC-korB* preceded by *ssb*, encoding ho-

		XylE activity [U]		
		vector	RepA	RepB
pMOB1.10.1	*xylE*	0.20	0.02	0.03
pMOB1.7.1	*xylE*	0.01	0.01	0.01
pMOB1.8.1	*xylE*	0.001	0.001	0.001
pMOB1.9.1	*xylE*	0.5	0.43	0.40
pPTOI		0.001	ND	ND

FIG. 6. Regulation of gene expression in the RA3 replication region. DNA fragments cloned into promoter probe vector pPTO1 and tested for promoter activity are shown. Units of XylE transcriptional activity were measured in extracts from IPTG-induced logarithmic-phase cultures of double transformants of C600K with pPTOI or its derivatives and expression vector pGBT30 and its derivatives pMOB1.5.1 (*tacp-repA*) and pMOB1.6.1 (*tacp-repB*). The results shown are averages from at least five experiments. ND, not determined.

mologs of single-stranded binding protein, and the downstream genes $orf22_{IPO2}$ and $orf14_{SB102}$, which are twice the length of *orf11* in RA3 (Fig. 7A). ORF22 and ORF14 seem to be conserved in amino acid sequence, whereas ORF11 of RA3 appears more distant evolutionarily.

The *kfr* locus of RA3 encodes two α-helical proteins, KfrA and KfrC, with putative auxiliary function in the segregation process, as shown for the IncP-1 equivalents (1, 16). As noted above, KfrA of RA3 includes a repetitive module of class I (residues 181 to 337) containing four repetitions of 36 amino acids with a fifth, incomplete, copy of 17 amino acids. The coiled-coil structure prediction for $KfrA_{RA3}$ performed with COILS (21) indicated that the repetitive part of KfrA is likely to form an α-helical structure (data not shown). KfrC, another α-helical protein that is 69% identical to the N-terminal part of KfrC from RK2, is encoded in the operon with *korC*, whereas the three Kfr proteins are encoded in one operon in IncP-1 plasmids.

KorC, KorA, and KorB (53 to 55% similar to the equivalent RK2 proteins) are predicted DNA-binding proteins, their homologs in IncP-1 plasmids acting as global regulators of gene expression in these plasmids (25, 38). The DNA-binding properties of the KorA and KorB proteins of RA3 have been confirmed (Kulinska and Jagura-Burdzy, unpublished).

KlcA, with 54% identity to the equivalent protein of RK2, might provide antirestriction protection, as has been suggested for KlcA of IncP-1α plasmids (20). The products of *orf02* and *orf04* of RA3 have no known homologs besides counterparts in pFBAOT6. However, BLAST searches revealed 45% identity over a stretch of 60 amino acids between the *orf02* product and the putative DnaA protein of *A. hydrophila*.

Conjugative transfer. Conjugative transfer functions in RA3 are encoded by a cluster of 21 genes organized in two operons, most of which have a high degree of sequence similarity (Table 2; see Table S1 in the supplemental material) to proposed conjugation gene products of environmental plasmids pXF51 (22), pIPO2 (37), and pSB102 (34) (Fig. 7B). The divergently transcribed tricistronic operon *orf34-orf36* encodes a putative integral membrane protein, a putative transcriptional regulator, and a protein with no homologs in the databases. The possibility that they are also involved in conjugative transfer cannot be excluded. By contrast with the IncP-1 *tra1* (*tra*) and *tra2* (*trb*) regions, the RA3 genes for the DNA-processing- and mating pair formation-associated components are not organized in separate blocks. Instead, the organization of the RA3 loci parallels that of pSB102; the relaxase gene (*nic*) is oriented divergently from the other transfer-associated genes, and a topoisomerase-encoding gene (*top*) is placed between mating pair formation genes coding for a putative cell wall hydrolase (*orf32*) and a putative major pilus subunit (*virB2*) (Fig. 7B). This arrangement also contrasts with the position of the topoisomerase gene *traE* in IncP-1α plasmid RP4, where *traE* is encoded between *traF* and *traD* in the DNA-processing gene cluster. Thus, RA3, pFBAOT6, pSB102, pXF51, and pIPO2 constitute a new organizational branch of conjugative transfer functions in environmental broad-host-range plasmids.

The location of the origin of transfer (*oriT*) of RA3 was first examined in silico on the basis of sequence homology between IncU representatives RA3 and pFBAOT6 and the *oriT* sites of pIPO2 (37), pSB102 (34), and pXF51 (22). This analysis suggested that *oriT* was situated in the long intergenic region upstream of *mobC* of RA3 (Fig. 2 and 7B). To examine this experimentally, a 458-bp restriction fragment encompassing the putative *oriT* (coordinates 9397 to 9854) was cloned into pMB1-based replicon pAKE600 (pAKB9.5) and introduced into *E. coli* DH5α (RA3). Conjugal-transfer mating experiments demonstrated the mobilization of pAKB9.5 into the CV601 recipient at a frequency of 2×10^{-2} transconjugant per donor (4×10^6 transconjugants), whereas mobilization of the pAKE600 vector was not detected under the same conditions. The mobilization frequency of pAKB9.5 was fivefold lower than the conjugation frequency of RA3. Plasmid DNA analysis of transconjugants confirmed the presence of two independent replicons.

Phenotypic traits. One-quarter of the RA3 plasmid (coordinates 32316 to 44457) constitutes the integration cassette. The module is highly similar to integration cassettes derived from two other IncU representatives, pAr-32 and pRAS1 (35) (Fig. 8A). The backbones (~35 kb) of IncU plasmids RA3 and pFBAOT6 vary by only seven nucleotide substitutions, one nucleotide deletion, and one nucleotide insertion but differ more dramatically in the amount and properties of more recently acquired genes (Fig. 8B). Thus, a different variable region was inserted into the same genetic context in RA3 and

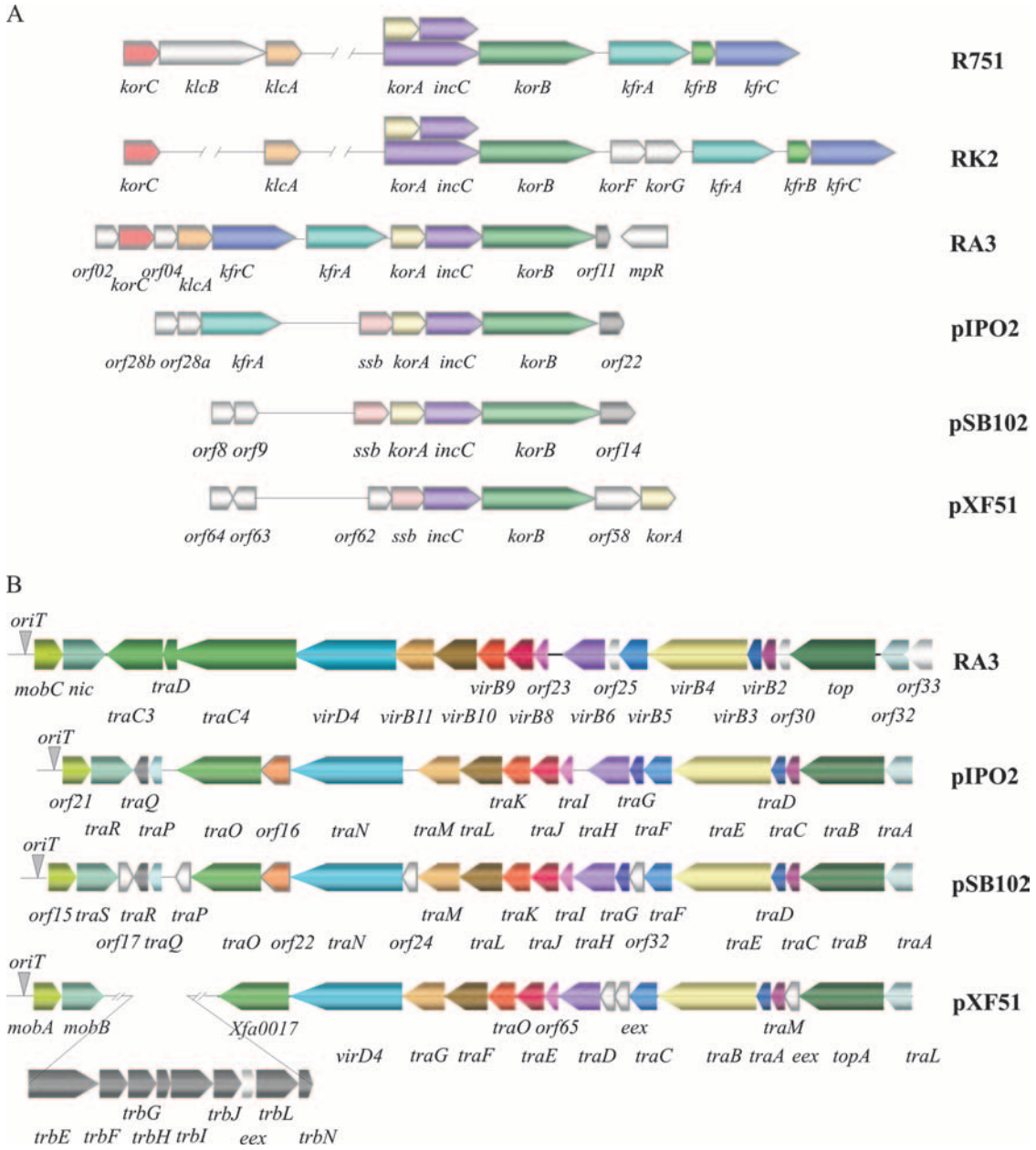

FIG. 7. Organization of maintenance and transfer modules in RA3 and its closest homologs. Comparison of the maintenance (A) and conjugative-transfer (B) regions of IncP-1 plasmids RK2 and R751, IncU plasmid RA3, and environmental broad-host-range plasmids pIPO2, pSB102, and pXF51. Arrows symbolize genes and directions of transcription. The same colors indicate homologous loci; ORFs which do not have a homolog in at least one plasmid are shown in white. The position of *oriT* is indicated by a grey inverted triangle.

pFBAOT6, between the replication and conjugative-transfer genes. Plasmid RA3 possesses a region of 10.5 kb that contains the class I complex integron with a CR1 element (*tnp513* associated with *catA2*) (41) located between partly duplicated 3′CSs (Fig. 8A). The IS*6100* insertion element has been transposed downstream of the 3′CS into a similar position as in pRAS1 (35) (Fig. 8A). In comparison, the variable region of pFBAOT6 encompasses ~54 kb and comprises IS*6100*, a class I integron (of a different length than in RA3 as it lacks one copy of the 3′CS and the CR1 element with *catA2*), and transposable elements, namely, a Tn*1721* composite transposon with Tn*3* (Fig. 8B). Analysis of sequences of both plasmids revealed that the extra sequence in pFBAOT6 is inserted following position 44968 of RA3, with duplication of the flanking nucleotides (TGTTGG). The transposon insertion in pFBAOT6 occurred in the region between *res* and about 50 bp before the repetitive region r1/r3, which, as described above, is potentially part of the plasmid replication module. The *res* genes of RA3 and pFBAOT6 show only 91% identity, which is much lower than for other parts of the plasmid sequences. Moreover, unlike pFBAOT6, RA3 does not include an IS*630* element inserted between *orf31* and *orf33* (note that the equivalent position in RA3

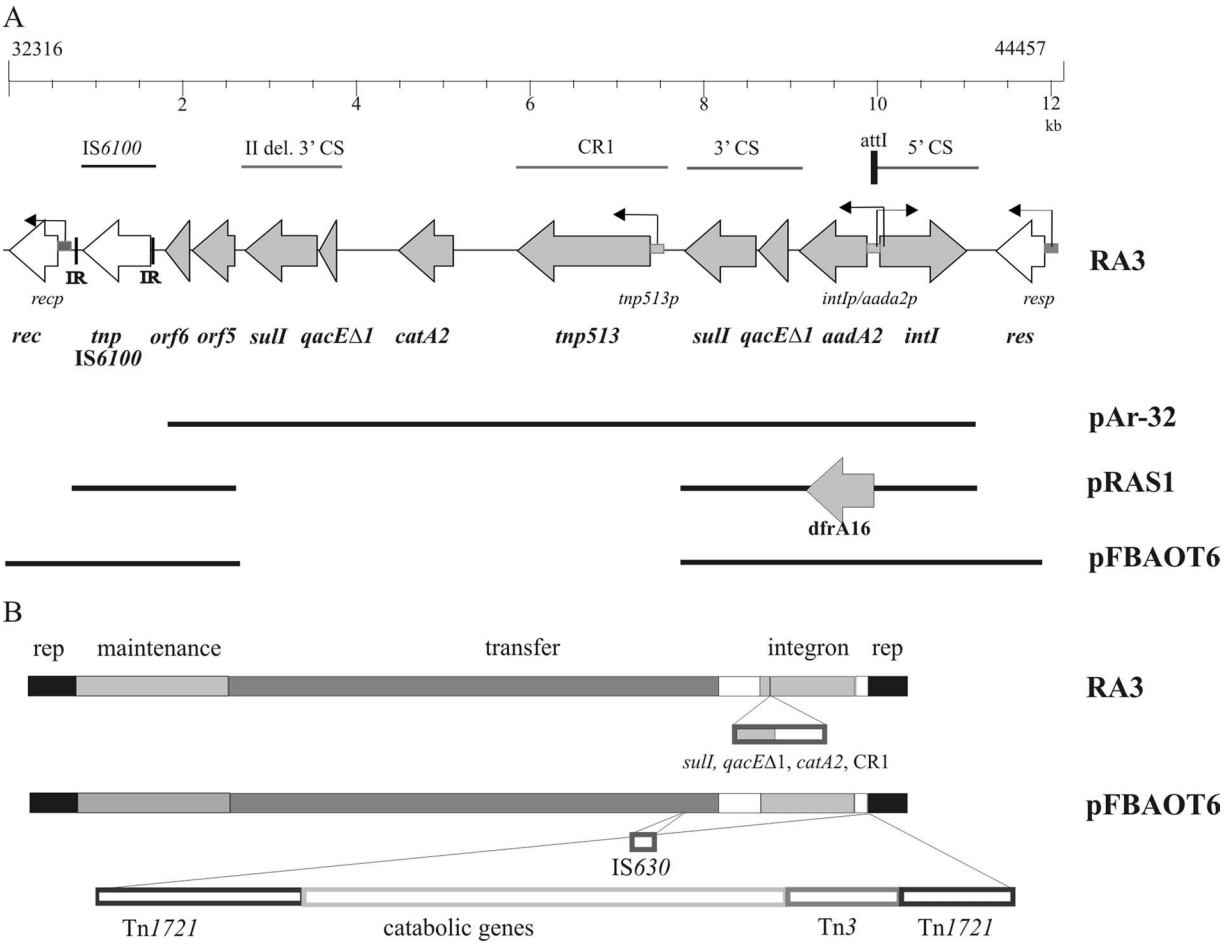

FIG. 8. Overview of the variable regions of IncU group representatives. (A) Schematic view of class I integrons based on the available sequence data of plasmids RA3 (DQ401103), pAr-32 (AJ517791), pRAS1 (AJ517790), and pFBAOT6 (NC_006143). Grey arrows mark the ORFs contained in the integron; white arrows indicate additional genes. The homologous regions present in different plasmids of the IncU group are marked. (B) Comparative genomic organization of IncU plasmids RA3 and pFBAOT6. Homologous blocks of genes are indicated by the same color; open rectangles represent nonhomologous components.

occurs between *orf32* and *orf33*, as *traD* was named *orf16* in RA3 instead of *orf15A* as in pFBAOT6).

The comparison of RA3 and pFBAOT6 is a notable example of how a plasmid backbone evolves by the acquisition of resistance and metabolic gene cassettes that enable the plasmid to succeed under variable conditions and under selective pressure after the commencement of broad antibiotic use. Since RA3 is only half of the size of pFBAOT6 with a significantly smaller variable region, it can be anticipated to constitute the incompatibility group U archetype, as previously suggested (6, 35).

Concluding remarks. Conjugative plasmid RA3 of the IncU incompatibility group is typical of the broad-host-range group of plasmids; it can self-transfer, replicate, and be stably maintained in alpha-, beta-, and gammaproteobacteria. Plasmid RA3 is characterized by a modular and mosaic structure with genes with defined properties clustered in functional blocks that have their closest homologs among plasmids from different incompatibility groups. For example, the maintenance module shows the highest level of relatedness to the maintenance region of IncP-1 plasmids, with 7 of 11 ORFs present in both plasmids, although the two regions differ markedly in gene organization. The partitioning operon of RA3 consists of *korA*, a short version of *incC* known as *incC2*, *korB*, and *orf11* of defined function. Three Kfr proteins specified by IncP-1 are limited to two in RA3, i.e., KfrA and KfrC, which apparently are encoded in separate transcription units. Similarly, KlcA, a putative antirestriction protein, is encoded separately from KorC in RA3, whereas the corresponding genes constitute a single operon in IncP-1 plasmids. Loci for *klcA* and *korC* are often found in plasmid replicons of diverse origins, e.g., in extended β-lactamase plasmid pCTXM-3 (9).

It was postulated that IncU plasmids constitute an evolutionarily narrow group in which plasmids possess a conserved backbone structure with a variable region confined to resistance-determining genes (2, 26, 35). The sequence conservation of the backbone functions between RA3 and pFBAOT6 is consistent with those suggestions, as only several nucleotide differences were found in the two plasmid backbones. However, classification of Rms149 into the IncU group (12) based on incompatibility testing and *rep* gene homology highlights a need to reexamine the notion of such strict conservation in the backbone functions of IncU group plasmids. The identity be-

tween RA3 and Rms149 is limited to the *rep* locus and *kfrA* (11). Moreover, the different requirements for the minimal replicons of the two plasmids, e.g., independence from DNA polymerase I for RA3 replication and different structures of putative replication origins in the two elements, indicate distinct evolutionary pathways. A wide diversity of beta- and gammaproteobacteria encode RepB homologs with 69 to 81% similarity (Fig. 5). Functional analysis of pRSB105, a dual replicon isolated from activated sludge from a wastewater treatment plant (33), indicated that its *rep1* locus provides the ability to replicate in gammaproteobacteria, whereas the *rep2* region that is homologous to the Rms149 replicon extends plasmid replication to betaproteobacteria. No ability to replicate in alphaproteobacteria was observed. As incompatibility studies have been pursued only with Rms149, pFBAOT6, and RA3, it is difficult to define the level of replication protein homology sufficient to exert incompatibility among IncU plasmids. However, it is likely that some of these newly sequenced replicons will be classified in the IncU group. Interestingly, all IncU replication proteins have variable C termini in which an HTH motif has been identified for both pFBAOT6 and RA3 (Fig. 5). A role for the intragenic r3 repeat was postulated in the initiation of Rms149 replication (12). However, this repeat is not sufficient for origin activity for RA3 (Fig. 3B). As the host range of RA3 seems to be the broadest among the related replicons tested, it may suggest an important role for the extended repetitive regions surrounding the *repA* and *repB* genes that are characteristic only of RA3. In conclusion, a main branch of IncU plasmids possesses a highly conserved core backbone with variable antibiotic resistance cassettes inserted at a common location. The widespread presence of the *repB*-based replication systems in mosaic plasmids of diverse origins suggests that this replication module is more common than previously realized.

ACKNOWLEDGMENTS

This project has been partially funded by grant PBZ-MNiSW-04/I/2007 (G.J.-B.). Work in the laboratory of F.H. is supported by grants from the Medical Research Council and The Wellcome Trust.

REFERENCES

1. **Adamczyk, M., P. Dołowy, M. Jonczyk, C. M. Thomas, and G. Jagura-Burdzy.** 2006. The *kfrA* gene is the first in a tricistronic operon required for survival of IncP-1 plasmid R751. Microbiology **152:**1621–1637.
2. **Adams, C. A., B. Austin, P. G. Meaden, and D. McIntosh.** 1998. Molecular characterization of plasmid-mediated oxytetracycline resistance in *Aeromonas salmonicida*. Appl. Environ. Microbiol. **64:**4194–4201.
3. **Aoki, T., S. Egusa, T. Kimura, and T. Watanabe.** 1971. Detection of R factors in naturally occurring *Aeromonas salmonicida* strains. Appl. Microbiol. **22:**716–717.
4. **Aoki, T., T. Kitao, N. Iemura, Y. Mitoma, and T. Nomura.** 1983. The susceptibility of *Aeromonas salmonicida* strains isolated in cultured and wild salmonids to various chemotherapeutants. Bull. Jpn. Soc. Sci. Fish. **49:**17–22.
5. **Bradford, M. M.** 1976. A rapid and sensitive method for the quantitation of microgram quantities of protein utilizing the principle of protein-dye binding. Anal. Biochem. **72:**248–254.
6. **Bradley, D. E., T. Aoki, T. Kitao, T. Arai, and H. Tschape.** 1982. Specification of characteristics for the classification of plasmids in incompatibility group U. Plasmid **8:**89–93.
7. **El-Sayed, A. K., J. Hothersall, and C. M. Thomas.** 2001. Quorum-sensing-dependent regulation of biosynthesis of the polyketide antibiotic mupirocin in *Pseudomonas fluorescens* NCIMB 10586. Microbiology **147:**2127–2139.
8. **Garnier, T., and S. T. Cole.** 1988. Complete nucleotide sequence and genetic organization of the bacteriocinogenic plasmid, pIP404, from *Clostridium perfringens*. Plasmid **19:**134–150.
9. **Gołebiewski, M., I. Kern-Zdanowicz, M. Zienkiewicz, M. Adamczyk, J. Zylinska, A. Baraniak, M. Gniadkowski, J. Bardowski, and P. Cegłowski.** 2007. Complete nucleotide sequence of the pCTX-M3 plasmid and its involvement in spread of the extended-spectrum β-lactamase gene $bla_{CTX-M-3}$. Antimicrob. Agents Chemother. **51:**3789–3795.
10. **Grigoriev, A.** 1998. Analyzing genomes with cumulative skew diagrams. Nucleic Acids Res. **26:**2286–2290.
11. **Haines, A. S., K. Jones, M. Cheung, and C. M. Thomas.** 2005. The IncP-6 plasmid Rms149 consists of a small mobilizable backbone with multiple large insertions. J. Bacteriol. **187:**4728–4738.
12. **Haines, A. S., M. Cheung, and C. M. Thomas.** 2006. Evidence that IncG (IncP-6) and IncU plasmids form a single incompatibility group. Plasmid **55:**210–215.
13. **Hanahan, D.** 1983. Studies on transformation of *Escherichia coli* with plasmids. J. Mol. Biol. **166:**557–580.
14. **Hayes, F.** 2003. Toxins-antitoxins: plasmid maintenance, programmed cell death, and cell cycle arrest. Science **301:**1496–1499.
15. **Hedges, R. W., and N. Datta.** 1971. fi^- R factors giving chloramphenicol resistance. Nature **234:**220–221.
16. **Jagura-Burdzy, G., and C. M. Thomas.** 1992. *kfrA* gene of broad host range plasmid RK2 encodes a novel DNA-binding protein. J. Mol. Biol. **225:**651–660.
17. **Jagura-Burdzy, G., J. P. Ibbotson, and C. M. Thomas.** 1991. The *korF* region of broad-host-range plasmid RK2 encodes two polypeptides with transcriptional repressor activity. J. Bacteriol. **173:**826–833.
18. **Kahn, M. R., R. Kolter, C. M. Thomas, D. Figurski, R. Meyer, E. Remault, and D. R. Helinski.** 1979. Plasmid cloning vehicles derived from plasmids ColE1, F, R6K, and RK2. Methods Enzymol. **68:**268–280.
19. **Koonin, E. V.** 1993. A superfamily of ATPases with diverse functions containing either classical or deviant ATP-binding motif. J. Mol. Biol. **229:**1165–1174.
20. **Larsen, M. H., and D. H. Figurski.** 1994. Structure, expression, and regulation of the *kilC* operon of promiscuous IncPα plasmids. J. Bacteriol. **176:**5022–5032.
21. **Lupas, A., M. Van Dyke, and J. Stock.** 1991. Predicting coiled coils from protein sequences. Science **252:**1162–1164.
22. **Marques, M. V., A. M. da Silva, and S. L. Gomes.** 2001. Genetic organization of plasmid pXF51 from the plant pathogen *Xylella fastidiosa*. Plasmid **45:**184–199.
23. **McKenney, K., H. Shimatake, D. Court, U. Schmeissner, C. Brady, and M. Rosenberg.** 1981. A system to study promoter and terminator signals recognized by *Escherichia coli* RNA polymerase. Gene Amplif. Anal. **2:**383–415.
24. **Mullis, K., F. Faloona, S. Scharf, R. Saiki, G. Horn, and H. Erlich.** 1986. Specific enzymatic amplification of DNA *in vitro*: the polymerase chain reaction. Cold Spring Harbor Symp. Quant. Biol. **51:**263–273.
25. **Pansegrau, W., E. Lanka, P. Barth, D. H. Figurski, D. G. Guiney, D. Haas, R. R. Helinski, H. Schwab, V. A. Stanisich, and C. M. Thomas.** 1994. Complete nucleotide sequence of Birmingham IncPα plasmids: compilation and comparative analysis. J. Mol. Biol. **239:**623–663.
26. **Rhodes, G., G. Huys, J. Swings, P. McGann, M. Hiney, P. Smith, and R. W. Pickup.** 2000. Distribution of oxytetracycline resistance plasmids between aeromonads in hospital and aquaculture environments: implication of Tn*1721* in dissemination of the tetracycline resistance determinant TetA. Appl. Environ. Microbiol. **66:**3883–3890.
27. **Rhodes, G., J. Parkhill, C. Bird, K. Ambrose, M. C. Jones, G. Huys, J. Swings, and R. W. Pickup.** 2004. Complete nucleotide sequence of the conjugative tetracycline resistance plasmid pFBAOT6, a member of a group of IncU plasmids with global ubiquity. Appl. Environ. Microbiol. **70:**7497–7510.
28. **Saeki, K., J. Hitomi, M. Okuda, Y. Hatada, Y. Kageyama, M. Takaiwa, H. Kubota, H. Hagihara, T. Kobayashi, S. Kawai, and S. Ito.** 2002. A novel species of alkaliphilic *Bacillus* that produces an oxidatively stable alkaline serine protease. Extremophiles **6:**65–72.
29. **Sambrook, J., E. F. Fritsch, and T. Maniatis.** 1989. Molecular cloning: a laboratory manual, 2nd ed. Cold Spring Harbor Laboratory Press, Cold Spring Harbor Laboratory, NY.
30. **Sandaa, R. A., and Ø. Enger.** 1994. Transfer in marine sediments of the naturally occurring plasmid pRAS1 encoding multiple antibiotic resistance. Appl. Environ. Microbiol. **60:**4234–4238.
31. **Sandaa, R. A., and Ø. Enger.** 1996. High frequency transfer of a broad host range plasmid present in an atypical strain of the fish pathogen *Aeromonas salmonicida*. Dis. Aquat. Org. **24:**71–75.
32. **Schaefer, C., and W. Messer.** 1991. DnaA protein/DNA interaction. Modulation of the recognition sequence. Mol. Gen. Genet. **226:**34–40.
33. **Schlüter, A., R. Szczepanowski, N. Kurz, S. Schneiker, I. Krahn, and A. Pühler.** 2007. Erythromycin resistance-conferring plasmid pRSB105, isolated from a sewage treatment plant, harbors a new macrolide resistance determinant, an integron-containing Tn*402*-like element, and a large region of unknown function. Appl. Environ. Microbiol. **73:**1952–1960.
34. **Schneiker, S., M. Keller, M. Droge, E. Lanka, A. Puhler, and W. Selbitschka.** 2001. The genetic organization and evolution of the broad host range mercury resistance plasmid pSB102 isolated from a microbial population residing in the rhizosphere of alfalfa. Nucleic Acids Res. **29:**5169–5181.
35. **Sørum, H., T. M. L'Abee-Lund, A. Solberg, and A. Wold.** 2003. Integron

containing IncU R plasmids pRAS1 and pAr-32 from the fish pathogen *Aeromonas salmonicida*. Antimicrob. Agents Chemother. **47:**1285–1290.

36. **Spratt, B. G., P. J. Hedge, S. de Heesen, A. Edelman, and J. K. Broome-Smith.** 1986. Kanamycin-resistant vectors that are analogues of plasmids pUC8, pUC9, EMBL8 and EMBL9. Gene **41:**337–342.
37. **Tauch, A., S. Schneiker, W. Selbitschka, A. Puhler, L. S. van Overbeek, K. Smalla, C. M. Thomas, M. J. Bailey, L. J. Forney, A. Weightman, P. Ceglowski, T. Pembroke, E. Tietze, G. Schroder, E. Lanka, and J. D. van Elsas.** 2002. The complete nucleotide sequence and environmental distribution of cryptic, conjugative, broad-host-range plasmid pIPO2 isolated from bacteria of wheat rhizosphere. Microbiology **148:**1637–1653.
38. **Thorsted, P. B., D. P. Macartney, P. Akhtar, A. S. Haines, N. Ali, P. Davidson, T. Stafford, M. J. Pocklington, W. Pansegrau, B. M. Wilkins, E. Lanka, and C. M. Thomas.** 1998. Complete sequence of the IncPβ plasmid R751: implications for evolution and organisation of the IncP backbone. J. Mol. Biol. **282:**969–990.
39. **Thorsted, P. B., D. S. Shah, D. Macartney, K. Kostelidou, and C. M. Thomas.** 1996. Conservation of the genetic switch between replication and transfer genes of IncP plasmids but divergence of the replication functions which are major host-range determinants. Plasmid **36:**95–111.
40. **Tian, Q. B., M. Ohnishi, A. Tabuchi, and Y. Terawaki.** 1996. A new plasmid-encoded proteic killer gene system: cloning, sequencing, and analyzing *hig* locus of plasmid Rts1. Biochem. Biophys. Res. Commun. **220:**280–284.
41. **Toleman, M. A., P. M. Bennett, and T. R. Walsh.** 2006. ISCR elements: novel gene-capturing systems of the 21st century? Microbiol. Mol. Biol. Rev. **70:** 296–316.
42. **Tschäpe, H., E. Tietze, and C. Koch.** 1981. Characterization of conjugative R plasmids belonging to the new incompatibility group IncU. J. Gen. Microbiol. **127:**155–160.
43. **Yanisch-Perron, C., J. Vieira, and J. Messing.** 1985. Improved M13 phage cloning vectors and host strains: nucleotide sequence of the M13mp18 and pUC19 vectors. Gene **33:**103–119.
44. **Zukowski, M. M., D. F. Gaffney, D. Speck, M. Kauffmann, A. Findeli, A. Wisecup, and J. P. Lecocq.** 1983. Chromogenic identification of genetic regulatory signals in *Bacillus subtilis* based on expression of a cloned *Pseudomonas* gene. Proc. Natl. Acad. Sci. USA **80:**1101–1105.